Ion-Induced DNA Structure Change in Nucleosomes†

Michael E. Hogan,* Bryan Hayes, and N. C. Wang
Department of Molecular Biology, Princeton University, Princeton, New Jersey 08544
Robert H. Austin
Department of Physics, Princeton University, Princeton, New Jersey 08544
Received January 27, 1986; Revised Manuscript Received April 23, 1986

ABSTRACT: Physical methods have been used to study calcium binding to the nucleosome core particle. Equilibrium dialysis of Ca^{2+} and spectroscopic analysis of a Ca^{2+} analogue show that the ion binds tightly to the particles, resulting in a significant change of DNA circular dichroism. This suggests that base stacking may be altered as a result of Ca^{2+} binding. In the presence of Ca^{2+}, the absorbance and fluorescence properties of methylene blue (MB), a DNA-specific intercalator, confirm that the dye binds tightly to nucleosomes by intercalation. However, secondary changes occur which suggest that the MB binding site is altered as a result of Ca^{2+} binding. Triplet state anisotropy decay and triplet lifetime quenching both show that in the Ca^{2+}–nucleosome complex, methylene blue is capable of wobbling over a substantial angular range at its binding site. To explain these data, it is proposed that Ca^{2+} binding to nucleosomes causes DNA to fold by means of a series of sharp bends (kinks). The properties of bound MB are best explained if it is presumed that the intercalator binds tightly to such kinked sites in the nucleosome. On the basis of these observations, we discuss the possibility that multivalent ion concentration in the nucleus is high enough that the smooth to kinked helix equilibrium may be near to its midpoint. Near such a midpoint, the secondary structure of DNA in the nucleosome might prove to be sensitive to effector molecule binding and to site-specific variation of DNA or histone composition within genes.

The nucleosome core particle is the fundamental structural subunit of eukaryotic chromatin. It is highly conserved evolutionarily and is found to contain two each of four histone proteins (H2A, H2B, H3, and H4) and a tightly associated DNA fragment 146 ± 2 base pairs long (McGhee & Felsenfeld, 1980). DNA in such particles is folded on the outside of a histone protein core to form $1^3/_4$ turn of left-hand solenoid, with a radius equal to 43 ± 2 Å (Richmond et al., 1984).

When free in solution, a DNA helix behaves as if it were a stiff elastic coil, with a persistence length near 200 base pairs (Kovacic & Van Holde, 1977). That stiffness specifies that to be folded smoothly in a nucleosome, approximately 50 kcal of bending work must be performed (by histones) upon the helix (Southwell, 1936).

Upon considering such energetics, Crick and Klug (1975), Sobell et al. (1977), and others (Zhurkin et al., 1979) have proposed that DNA in a nucleosome might relax into a discontinuously folded (kinked) helix geometry to relieve that bending stress. Although the structure models which have been described for such a kink differ in detail, each predicts the loss of one base stacking interaction at a kink site. Such unstacking entails a large positive free energy change (probably near +10 kcal). Consequently, even though a kink is a rare event in linear DNA, such an equilibrium between a B form and kinked helix secondary structure might be favorable in a nucleosome if it can liberate the energy stored in DNA as bending stress.

Recently, a structure for the nucleosome core particle has been resolved by X-ray diffration to 7-Å resolution in crystals (Richmond et al., 1984). DNA in those nucleosome crystals displays two types of folded helix geometry: smooth deformation over much of the helix, separated by four sites with a severe discontinuous bend.

In light of the energetic arguments presented above, and the mixed bending geometry evident in the available nucleosome crystal structure, we have considered the possibility that at mild conditions in solution, the energy of a helix folded by kinks may be so similar to that of a stressed, smoothly deformed structure that the two alternative conformations may equilibrate with one another. Here, we explore the possibility that a simple, biologically relevant effector molecule might bind to the nucleosome and shift that equilibrium.

We have pursued this hypothesis using biochemical and biophysical methods to study the binding of the effector molecule Ca^{2+} to highly purified nucleosome core particles. Equilibrium dialysis methods have been employed to monitor the affinity and stoichiometry of ion binding. Circular dichroism (CD) has been used to monitor DNA stacking change in the particles. Absorbance and luminescence methods (fluorescence, triplet state anisotropy decay, and triplet state quenching) have been used to monitor the distribution of dye probe molecules upon the nucleosome and general features of the binding site.

Independent of any particular model, the data indicate that as a result of Ca^{2+} binding to a nucleosome, its DNA experiences significant secondary structure change. In contrast, linear DNA is not similarly affected by Ca^{2+} binding.

Materials and Methods

Preparation of Nucleosome Core Particles. Nucleosome core particles were prepared by a modification of techniques described previously (Wang et al., 1982). Briefly, nuclei were isolated from mature chicken erythrocytes by repeated washing with 150 mM NaCl, 15 mM sodium cacodylate, pH 7.2, 1 mM $CaCl_2$, 0.1 mM phenylmethane sulfonyl fluoride (PMSF), 0.1 mM tosyl-L-lysine chloromethyl ketone (TLCK), and 5 mM sodium butyrate. Nuclei were then digested with micrococcal nuclease (0.2 unit/mg of DNA) for 20 min at 37 °C in 170 mM KCl, 10 mM piperazine-*N*,*N*′-bis(2-ethane-

† This work was supported by Grant PCM-8402776 from the National Science Foundation (to M.E.H.) and by Grant GM 30789 from the National Institute of General Medical Science (to R.H.A.).

0006-2960/86/0425-5070$01.50/0

sulfonic acid) (PIPES), 5 mM $CaCl_2$, and 10% sucrose, pH 7.2. Approximately 50% of the nucleosome subunits liberated by the enzyme remain insoluble in that buffer. The soluble fraction which perfuses from the nucleus was harvested by centrifugation and was partially purified and desalted by chromatography through a Sepharose 6B resin, eluting with 10 mM tris(hydroxymethyl)aminomethane (Tris), 1 mM ethylenediaminetetraacetic acid (EDTA), 0.1 mM PMSF, and 0.1 mM TLCK, pH 7.8. Fractions containing nucleosome particles were then pooled, concentrated by pressure filtration (Amicon PM10 membrane), and then fractionated by preparative column electrophoresis (Savant Instruments) on a 6% polyacrylamide gel.

DNA fragments (146 base pairs long) were isolated from purified nucleosomes by digestion with proteinase K (1 μg of protease/10 μg of DNA at 37 °C for 2 h), followed by three phenol extractions. DNA was then fractionated over a Sepharose 6B resin to eliminate small molecular weight contaminants which may have accumulated during deproteination.

Histones were analyzed on 15% acrylamide–0.5% bis(acrylamide)/sodium dodecyl sulfate (SDS) gels, staining with Coomassie Blue. DNA and nucleosome particles were analyzed on 6% acrylamide gels, calibrated relative to the *Hae*III digest of pBR322.

Equilibrium Dialysis. Ca^{2+} binding was monitored by equilibrium dialysis in 10 mM Tris-HCl at 4 °C, using $^{45}CaCl_2$ as a probe (NEN). Nucleosome concentration in these experiments was determined photometrically, assuming ϵ_{260} = 6500 cm^{-1} M^{-1} (bases) and the measured value of 292 base equivalents per particle. Samples were allowed to equilibrate for 36 h prior to analysis. In no instance was proteolysis or DNA degradation detected after such treatment.

Spectroscopy. Fluorescence measurements were performed on an Perkin-Elmer fluorometer. CD measurements were performed on an Aviv spectropolarimeter, made available by the Rutgers Chemistry Department. Absorbance measurements were performed on an HP8450 dual-beam spectrometer. We have noticed that residual EDTA dialyzes slowly from nucleosome samples. Consequently, samples were dialyzed for spectroscopic measurements at least 36 h (10 mM Tris-HCl, pH 7.2).

Triplet Absorbance and Anisotropy. We have made substantial improvements in the time response from previous measurements (Wang et al., 1982), in particular the use of a small nitrogen laser-driven dye laser (Photochemical Research Associates, Oak Ridge, TN) as an oscillator. The pulse width from this laser is approximately 200 ps. The output pulse from the oscillator is amplified by dye cells pumped by a frequency-doubled Nd/YAG laser. Details of this technique are described elsewhere (Austin & LeGrange, 1985). The final time response of the system was ultimately determined by the 4-ns rise time (10–90%) of a Biomation 6500 transient recorder. All other aspects of the apparatus are as detailed in previous experiments (Wang et al., 1982; Berkoff et al., 1986).

In previous work, where we have employed methylene blue (MB) as a dye probe, we have noted that the singlet depletion signal (the anisotropy decay signal) in those measurements is always smaller in magnitude than the maximum value (0.40) predicted for a linear chromophore (Wang et al., 1982). Kinosita and colleagues have shown that a signal reduction of that kind can result from fast, undetected motions of the dye probe, from the superposition of perpendicular transition moments in the dye absorption spectrum, or from saturation effects due to irradiation with an intense laser light source (Kawato & Kinosita, 1981).

In order to characterize MB signal amplitudes in our anisotropy decay measurements, we have measured the anisotropy of MB, embedded in a rigid glass matrix of DL-arabinose. In such a matrix, we find that measured initial anisotropy values are identical with those which we measure for MB–DNA complexes and are independent of the intensity of the exciting light source (data not shown). This outcome confirms that the initial anisotropy values which we measure (0.25) are *not* reduced due to fast undetected motion of the dye probe or by saturation effects due to the intense laser source.

Therefore, measured anisotropy values for MB must be reduced as a result of the superposition of perpendicular absorbance transition moments. As will be discussed later in the text, at the wavelengths we have monitored, MB absorbance does in fact result from two overlapping absorbance transitions. As we will show in another paper, reduced dye probe anisotropy signals are directly related to that overlap.

Results

Ca^{2+} Binds Tightly to Nucleosomes. Nucleosome particles for ion binding are well-defined: they contain equal amounts of the four core histones and are free from any detectable histone degradation or contamination with extraneous protein. They contain a fragment of DNA which is 146 ± 2 bases long. The particle migrates as a well-defined electrophoretic species [see Wang et al. (1982) for detailed characterization]. The integrity of the particle or its components is not altered by extended dialysis at 4 °C against a Ca^{2+} concentration as high as 500 μM (not shown).

Figure 1A contains Scatchard plots for Ca^{2+} binding to such nucleosomes measured by equilibrium dialysis (lower curve). For comparison, we have also measured Ca^{2+} binding to linear 146 base pair (bp) DNA purified from the particles (upper curve). As seen, Ca^{2+} binding to 146 bp DNA is fit very well by the Manning theory (Friedman & Manning, 1984) for nonspecific counterion condensation with a B DNA helix, as expected from several other studies (Clement et al., 1973). In contrast, Ca^{2+} binding to the nucleosome is more complicated (lower curve). The Scatchard representation of the data is curved, which is indicative of multiple binding sites, or anticooperative binding. For simplicity, and in light of data presented below, we have chosen to catalog these data in terms of a simple two-site binding model of the form:

$$\frac{r}{c} = \frac{n_1 K_1}{1 + K_1 c} + \frac{n_2 K_2}{1 + K_2 c} \quad (1)$$

where r is the ratio of bound ion concentration to total nucleosome concentration, c the concentration of free ions, n_i the number of binding sites per base equivalent, and K_i the association constant for each binding site class.

A fit of eq 1 to the data is presented as a solid line in Figure 1A. In the context of that fit, there appear to be 0.05 tight site per base equivalent or approximately 15 per nucleosome, with an apparent association constant $\sim 4.0 \times 10^5$ M^{-1}. That calculated affinity is greater than that measured for uncomplexed DNA (compare initial slopes of the binding data in Figure 1A). In the context of such a two-site model, the second class of Ca^{2+} binding site in the nucleosome is characterized by an association constant near 3.0×10^3 M^{-1} which is very similar to that measured for uncomplexed DNA (compare final slopes of the binding data).

It is important to emphasize that these particles are free from linker DNA segments and have been subjected to exhaustive purification during isolation. Consequently, the high-affinity Ca^{2+} binding process which occurs at low satu-

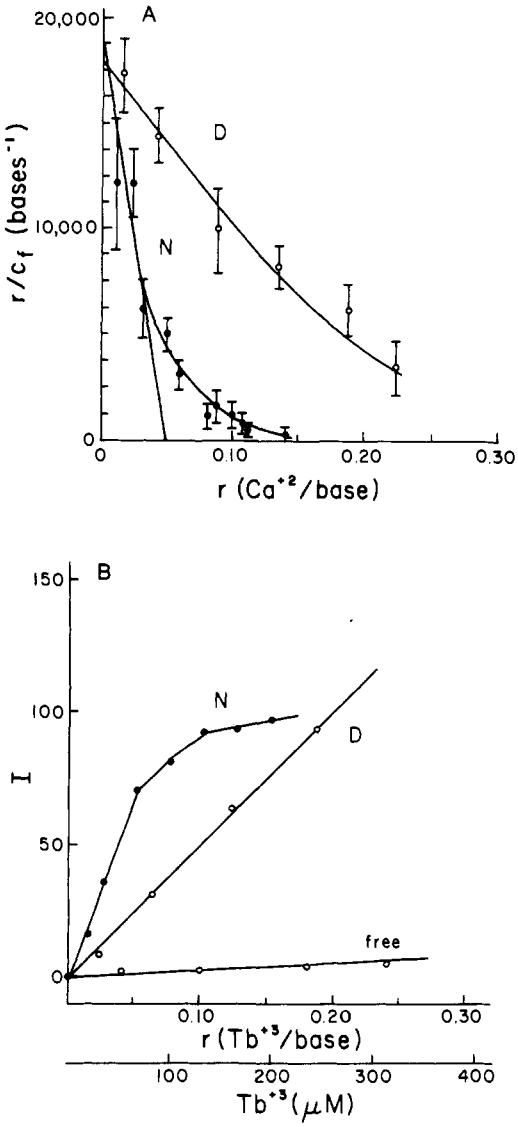

FIGURE 1: Ca^{2+} and Tb^{3+} binding to nucleosomes. (A) Ca^{2+} binding has been monitored by dialysis against 10 mM Tris-HCl, pH 7.2 at 4 °C, as described under Materials and Methods, and then displayed as a Scatchard plot. Data have been measured over a substrate concentration range from 2×10^{-4} to 1.5×10^{-3} M bases. No systematic substrate concentration dependence could be detected in that range. Error bars correspond to one standard deviation from the mean of four or more independent measurements. (Open circles) Ca^{2+} binding data for 146 bp DNA helices. (Closed circles) Ca^{2+} binding data for nucleosome core particles. The curve through the 146 bp DNA data (D) corresponds to the low saturation limit of the Manning theory for divalent counterion condensation to B DNA in the presence of 10 mM supporting monovalent cation (Friedman & Manning, 1984). The line drawn through the early portion of the nucleosome data (N) corresponds to a fit of the low saturation data to a two-state model which specifies one high-affinity class of Ca^{2+} binding site per 20 bases (see eq 1 in the text). (B) Base to Tb^{3+} energy transfer as monitored by Tb^{3+} luminescence (exciting at 295 nm, monitoring at 545 nm). Data have been monitored in 10 mM Tris-HCl, pH 7.2, 4 °C, at 1.3×10^{-3} M substrate concentration (bases). To facilitate comparison between the steady-state fluorescence yield of bound and free Tb^{3+}, data have been corrected for absorbance of the DNA substrate at 295 nm. In each instance, corrected fluorescence (I) has been plotted as a function of added $TbCl_3$ concentration. (Top curve) Tb^{3+} complexes (N) with nucleosome core particles. (Middle curve) Tb^{3+} complexes with linear 146 bp DNA (D). (Bottom curve) Free Tb^{3+}, in the absence of substrate. For nucleosome and 146 bp DNA complexes, substrate concentration is identical; therefore, each may also be cataloged in terms of added Tb^{3+} concentration per base equivalent. The upper horizontal axis corresponds to that characterization of the data.

ration is a property of the nucleosome core and is not related to contaminating DNA segments.

DNA to Terbium Ion Energy Transfer. To investigate the possibility that Ca^{2+} binding to nucleosomes is biphasic, we have used fluorescence methods to monitor the binding of Tb^{3+} ion to nucleosomes. Tb^{3+} is a luminescent Ca^{2+} analogue which binds tightly to proteins and to nucleic acids. Tb^{3+} can substitute for Ca^{2+} in tRNA (Kayne & Cohn, 1974) and Ca^{2+} transport proteins (Martin, 1983). On the basis of the biological similarity of the ions (and based upon data discussed below), it is likely that Tb^{3+} and Ca^{2+} could bind to the same site within a nucleosome. In that instance, Tb^{3+} luminescence can be used to monitor the physical properties of Ca^{2+} binding sites.

When irradiated at 295 nm, free Tb^{3+} is weakly fluorescent. However, when bound to nucleic acids, energy transfer can occur between the base heterocycle and the ion, giving rise to strong Tb^{3+} luminescence at 545 nm (Topal & Fresco, 1980). Moreover, since amino acid absorbance is negligible at 295 nm, enhanced luminescence of bound Tb^{3+} can be used to discriminate protein from nucleic acid binding sites, since under these experimental conditions, protein-bound Tb^{3+} ions will not experience efficient energy transfer (histone absorbance is indetectible at 295 nm).

In Figure 1B, we display base to Tb^{3+} energy transfer efficiency (monitored as enhanced Tb^{3+} luminescence) as a function of increasing Tb^{3+} concentration. For nucleosomes and for 146 bp DNA, substrate concentration had been adjusted so that over the range of Tb^{3+} ion concentrations tested, halving the nucleotide concentration had no effect on transfer efficiency (not shown) which confirms that the changes which are measured are due exclusively to bound Tb^{3+} ion.

In the range from 0 to 0.05 bound Tb^{3+} per base equivalent, the fluorescence yield per bound ion is constant and approximately 2.5 times greater for nucleosomes than for 146 bp DNA (Figure 1B). Such enhanced Tb^{3+} fluorescence confirms that Tb^{3+} binds to DNA in the nucleosome (and not to histones) at low ion density. Because the efficiency of energy transfer to Tb^{3+} is dominated by the base to Tb^{3+} separation (Stryer et al., 1982; Geladē & De Schryver, 1984), these data also suggest that when bound to DNA in the nucleosome, Tb^{3+} binding site structure may be different than in a linear helix.

At bound ion densities above 0.05 per base, the mode of Tb^{3+} binding appears to change, as evidenced by a decrease in the base to ion transfer rate (Figure 1B). Such an apparent difference in Tb^{3+} binding at high ion density is consistent with the two-site interpretation of the Ca^{2+} binding isotherm in Figure 1A.

The quantitative relation between energy transfer efficiency and Tb^{3+} binding site structure has been the object of several studies (Geladē & De Schryver, 1984; Stryer et al., 1982; Horrocks et al., 1980). As summarized by Stryer (Stryer et al., 1982), for many donors, transfer to Tb^{3+} may be dominated by an electron overlap (a direct contact) interaction when separation is less than 5 Å but appears to be a predominantly dipolar (throughspace) process for separation in the 10–30-Å range. Transfer due to a contact interaction decreases exponentially with separation, while dipolar transfer decreases as the sixth power of distance (Stryer et al., 1982). Consequently, in the most general case, the steady-state fluorescence which results from DNA to Tb^{3+} energy transfer can have a complicated distance dependence. That dependence becomes simpler in a variety of specific limiting models. Below, we discuss Tb^{3+} energy transfer in the context of such a model.

Taken together, the two classes of binding data which are displayed in Figure 1 suggest that there may be a class of DNA binding site in the nucleosome which is different than that seen in a linear helix. Below, we now describe how this tight ion binding process affects DNA structure in the nucleosome.

CD Measurements. Although circular dichroism is difficult to interpret in terms of specific conformational models, the technique has proven to be a useful method to detect conformational change in proteins and nucleic acids. The method is particularly useful in chromatin, because the histones contain few aromatic side chains and for that reason do not contribute significantly to circular dichroism spectra of chromatin in the range from 250 to 300 nm (Cowman & Fasman, 1978).

Figure 2A contains circular dichroism spectra of nucleosome particles. In the absence of Ca^{2+} (top curve), the measured spectrum is as expected from published values for nucleosome cores (Cowman & Fasman, 1978). However, in the presence of 500 μM Ca^{2+}, the spectrum changes substantially. As seen in Figure 2A (insert), that change is well characterized as a single negative component with a maximum near 280 nm. Ca^{2+} does not produce a CD change of that kind when bound to purified 146 bp DNA (Figure 2B). Evidently, the change monitored by CD is specific to DNA when wrapped as a nucleosome.

As seen in Figure 2A, the Ca^{2+}-induced ellipticity decrease at 280 nm is complete by 500 μM Ca^{2+}. Using the nucleosome concentration in these experiments (legend to Figure 2), and the binding data of Figure 1A, we calculate that this end point corresponds to a bound ion density of 0.13 Ca^{2+} per base, at a free Ca^{2+} concentration of 450 μM. That end point, as monitored by CD, corresponds closely to saturation of the Ca^{2+} sites monitored by dialysis or by Tb^{3+} luminescence, suggesting a direct correspondence between DNA structure change and Ca^{2+} binding to its highest affinity sites.

In Figure 2A, we also display an important control experiment. Sodium chloride has been added to nucleosomes in standard Tris buffer. As seen, the CD spectrum of nucleosomes is unaffected by 10 mM monovalent ion. Such monovalent ion independence suggests that the change induced by Ca^{2+} binding is not a simple ionic effect but instead must result from a specific interaction between Ca^{2+} and the nucleosome. Work below confirms this observation.

Dye Probe Binding Measurements with Methylene Blue. Both theory (Platt, 1949) and experiment (Albert, 1966) show that the absorbance spectrum of a planar heterocyclic dye may be composed of multiple transitions. The transition dipoles responsible for those bands tend to be parallel to the aromatic plane, but orthogonal to each other with a direction which alternates as a function of wavelength: often, the longest wavelength transition is parallel to the longest molecular axis, while the next longest is directed along the short axis.

As expected from its structure, the absorbance spectrum of methylene blue (MB) falls into that general class. MB has two strong absorbance bands in the visible, one at 662 nm and a second near 620 nm which is evident as a pronounced shoulder on the spectrum. The absolute polarization of those two transitions has not been determined for MB. However, for proflavin, a structural analogue of MB, the equivalent absorbance transitions are orthogonal, and, as expected, the longest wavelength transition is directed along the long dye axis (Wittwer et al., 1959). It is possible that MB displays similar polarization of its absorbance moments.

Intercalating dyes bind tightly to DNA when it is folded to form a nucleosome (Wang et al., 1982; Wu et al., 1980; Watanabe et al., 1983). At low probe density (less than five or six bound molecules per nucleosome), ethidium bromide appears to leave nucleosome structure intact, intercalating specifically into the helix to produce a bound dye complex which is nearly indistinguishable from that formed with linear DNA, as determined by absorbance (Wu et al., 1980), steady-state fluorescence (Wu et al., 1980), and fluorescence anisotropy (Watanabe et al., 1983) of the bound dye.

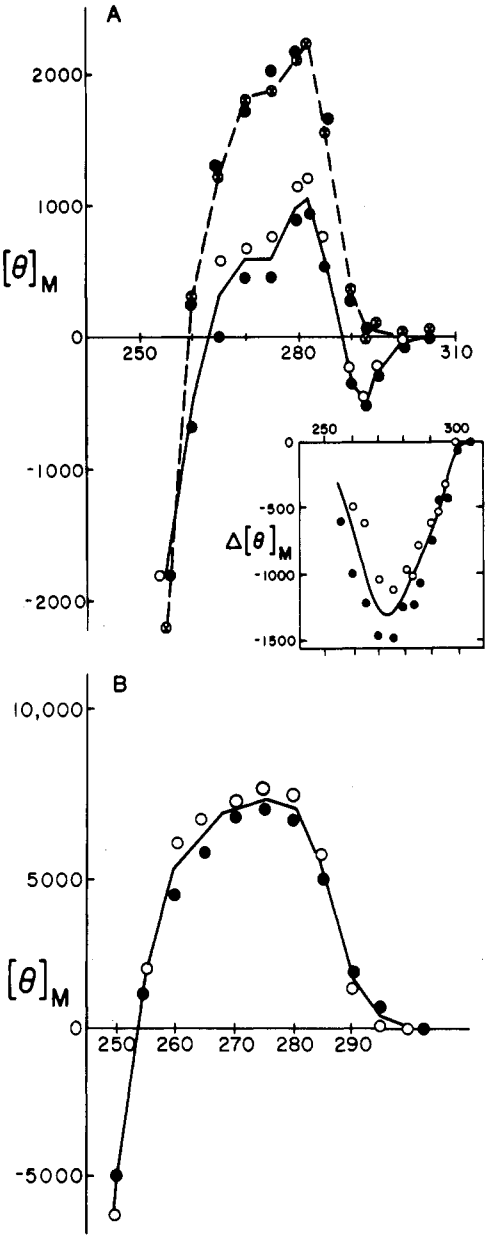

FIGURE 2: Circular dichroism of Ca^{2+}–nucleosome complexes. CD measurements have been monitored as described under Materials and Methods in 10 mM Tris-HCl, pH 7.2, 4 °C, to which had been added the specified concentration of $CaCl_2$ or NaCl. Substrate concentration was held constant at 1.3×10^{-4} M (bases). Data have been plotted as a molar ellipticity (deg M^{-1} cm^{-1} × 0.01) in base concentration units. (A) CD measurements on nucleosome core particles. (Top curve) Ellipticity measurements in the absence of Ca^{2+} (open circles) or in the presence of 10 mM NaCl (closed circles). (Bottom curve) Ellipticity measurements in the presence of 500 μM total Ca^{2+} (closed circles) or 1 mM total Ca^{2+} (open circles). (Insert) Ellipticity change which occurs upon binding Ca^{2+}: (closed circles) 500 μM Ca^{2+}; (open circles) 1000 μM Ca^{2+}. (B) CD measurements on uncomplexed 146 bp DNA. (Open circles) No added Ca^{2+}; (closed circles) 500 μM added Ca^{2+}. For nucleosome and linear DNA measurements, the data which have been displayed correspond to a numerical mean of four independent measurements, with the buffer contribution subtracted away.

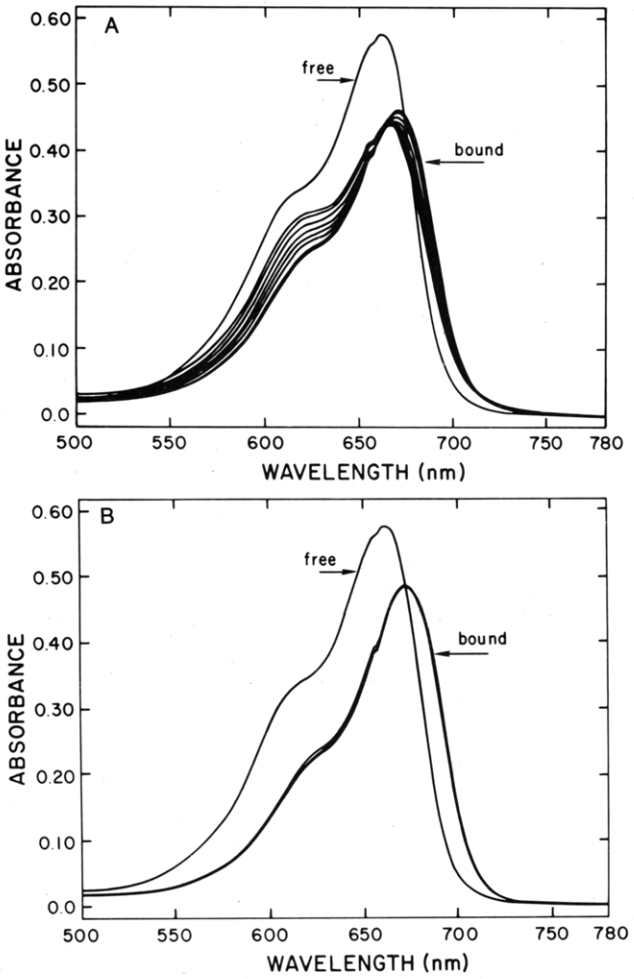

FIGURE 3: Absorbance measurements of methylene blue complexes with nucleosomes. Measurements have been performed at a limiting, high substrate concentration (1.31×10^{-3} M bases); i.e., measurements performed at a 2-fold dilution of dye and substrate gave identical spectra, which confirms that dye probe dissociation does not contribute to these data (not shown). Measurements were made at 4 °C in 10 mM Tris-HCl, pH 7.2. (A) Ca^{2+} titration of the MB–nucleosome complex at a dye to nucleosome ratio equal to one. (Top curve) Free MB in solution, 4.5×10^{-6} M. (Bottom curves) MB at 4.5×10^{-6} M bound to the nucleosome as a function of added Ca^{2+} concentration: 0, 100, 198, 398, 496, 590, 880, and 1212 μM. Absorbance curves decrease with added Ca^{2+} at 690 nm and increase when measured at 620 nm. (B) Ca^{2+} titration of the MB–146 bp DNA complex at a dye to helix ratio of one. (Top curve) Free MB at 4.5×10^{-6} M. (Bottom curves) MB bound to 146 bp DNA as a function of added Ca^{2+} concentration: 0, 298, and 880 μM added Ca^{2+}. As seen, Ca^{2+} has little effect on the spectrum of MB–DNA complexes.

Methylene blue (MB) is another example of such an intercalator. As we have shown previously, the fluorescence yield, absorbance, linear dichroism, binding affinity, and triplet state polarization decay of MB when bound to nucleosomes are similar to those measured for linear DNA helices in the absence of divalent ions (Wang et al., 1982). Here, we take advantage of this dye probe to monitor the effects of Ca^{2+} binding to nucleosomes.

In Figure 3A, it can be seen that in the absence of added Ca^{2+} the absorbance of MB when bound to the nucleosome is similar to that of its complex with linear DNA (Figure 3B). In both cases, the dye experiences a 26% decrease in absorbance at the principle absorbance maximum (662 nm) and a 35% absorbance decrease at its second absorbance band (620 nm). Such hypochromism is seen for all intercalating dyes and, as expected from theory, is diagnostic for the strong vertical stacking interactions which occur between the dye and the DNA bases in an intercalated complex (Bush, 1974).

In Figure 3B, it can be seen that Ca^{2+} has no effect on the absorbance of MB bound to linear DNA. However, over the same Ca^{2+} concentration range, the absorbance spectrum of MB bound to nucleosomes changes significantly (Figure 3A). Several general features of these Ca^{2+}-induced changes should be noted.

(a) The extinction coefficient of the principle MB absorbance band decreases by 5% as a result of Ca^{2+} binding, suggesting that as visualized by hypochromism of the 662-nm transition, Ca^{2+} appears to increase the MB stacking interaction with the helix.

(b) The Ca^{2+}-induced spectral changes which occur in the nucleosome have a well-defined isosbestic point at 662 nm. Since that wavelength also corresponds to the absorbance maximum of the free dye, an isosbestic point at 662 nm confirms that at the high substrate concentration used in these experiments, the measured absorbance change is not due to dissociation of the dye from the nucleosome. Such tight binding at all measured Ca^{2+} concentrations is confirmed by explicit MB binding measurements described in Figure 5.

(c) The Ca^{2+} transition monitored by absorbance displays Ca^{2+} binding saturation above 500 μM total Ca^{2+}, at 1.3×10^{-3} M bases. As seen from CD measurements, that Ca^{2+} concentration dependence is as expected if saturation of tight Ca^{2+} binding sites is responsible for the transition.

(d) The presence of an isosbestic point at 662 nm indicates that MB is distributed among two classes of site: one which is similar (spectrally) to binding sites measured in the absence of Ca^{2+} and a second class of sites which arises as a result of ion binding. That interpretation is confirmed by triplet state measurements described below.

(e) Ca^{2+} binding to nucleosomes induces a 27% *increase* in MB absorbance at 620 nm, with a dose response which is identical with that measured at longer wavelengths. As discussed, it is most likely (but not proven) that the transition dipole moment responsible for MB absorption at 620 nm is positioned along the short axis of the dye and is perpendicular to that which gives rise to absorbance at 662 nm (Kern & Doerr, 1961). Both lie within the plane of the dye, as is customary for the principle π–π^* transitions of aromatic rings.

The general theory of hypochromism predicts that for a chromophore with two absorbance transitions, each transition will respond independently to stacking interactions with a neighboring heterocycle (Bush, 1974). In the context of that general observation, the data in Figure 3 suggest that, as a result of Ca^{2+} binding to nucleosomes, MB becomes bound to sites where the long dye axis is stacked vertically upon its neighboring bases but the short axis of the dye is unstacked compared to a binding site in a linear DNA helix.

Fluorescence Measurements. The fluorescence yield of bound intercalators has proven to be a sensitive measure of binding site secondary structure in helices (LePecq & Paoletti, 1967). As is the case for most intercalators, MB experiences a major quenching of its fluorescence when it intercalates into DNA due to stacking interactions and solvent exclusion by the neighboring base planes (Wang et al., 1982). Here we take advantage of that characteristic change to monitor the Ca^{2+}-induced change of those binding site interactions in the nucleosome.

As seen in Figure 4, in the absence of Ca^{2+}, the fluorescence yield of MB bound to nucleosomes is 0.21 time that of the free dye. That decrease is similar to the change measured when MB is bound to linear DNA (Figure 4, lower curve) as determined previously (Wang et al., 1982).

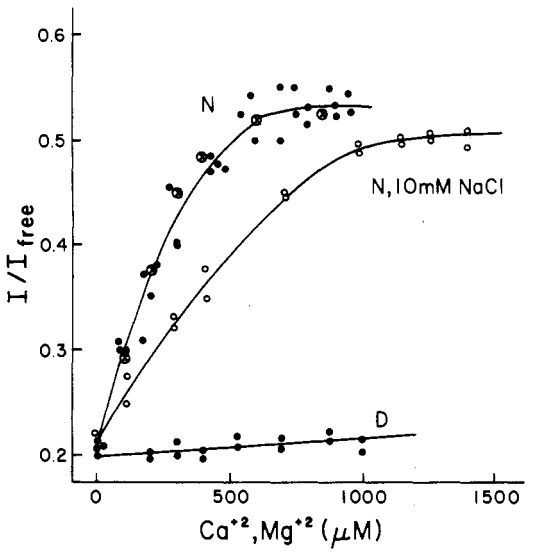

FIGURE 4: Fluorescence measurements of MB complexes with nucleosomes. Characteristic MB fluorescence (exciting at 665 nm, monitoring at 685 nm) has been measured as a function of added Ca^{2+} concentration at a substrate concentration of 1.31×10^{-3} M (bases). The ratio of bound dye molecules to particles is held constant at 1.0. All other conditions are as described in the legend to Figure 3. In each instance, fluorescence yield has been measured, relative to the value measured for the free dye under identical conditions (I/I_{free}). (Top curve, closed circles) Relative fluorescence yield of the MB–DNA complex (N) as a function of added Ca^{2+} concentration. [Top curve, circles inscribed with a (×)] relative fluorescence yield as a function of added Mg^{2+} concentration. (Middle curve) Relative fluorescence of the MB–nucleosome complex as a function of added Ca^{2+} concentration in the presence of 10 mM added NaCl in addition to 10 mM Tris-HCl. (Bottom curve) Relative fluorescence of the MB complex with linear 146 bp long DNA (one bound MB per helix).

Upon addition of Ca^{2+}, the fluorescence of MB bound to nucleosomes increases by a factor of 2.5 (Figure 4, upper curves). In contrast, MB bound to linear DNA is unresponsive to such Ca^{2+} addition (Figure 4, lower curve). We have determined that this fluorescence increase is independent of nucleosome concentration above 6×10^{-4} M bases (not shown) and, therefore, is independent of dye dissociation from the complex. The Ca^{2+}-induced transition saturates near 500 μM added Ca^{2+}, again consistent with the idea that the tight binding of Ca^{2+} is responsible for the transition.

Interestingly, Na^+ appears to be a weak inhibitor of the transition, i.e., as seen in Figure 4 (middle curve), the midpoint of the Ca^{2+}-induced transition is shifted from 200 to 450 μM total Ca^{2+} in the presence of 10 mM total Na^+. This Na^+ effect suggests that the effect of this ion is to weaken Ca^{2+} affinity to the nucleosome electrostatically, without itself inducing the structure transition in the nucleosome.

The magnitude of the dye fluorescence increase which accompanies Ca^{2+} binding cannot be used to define a structure model by itself. However, the 2-fold quenching of MB fluorescence which occurs when it binds to the Ca^{2+}-saturated nucleosome suggests that MB continues to experience interactions with the helix of the sort which are inferred from the absorbance changes we have monitored (Figure 3). Both sets of spectral data are consistent with the idea that in the presence of saturating Ca^{2+} concentration, MB continues to bind to nucleosomes by intercalating into the helix, although forming a complex where details of binding site structure must be different than for linear DNA.

Dye Probe Binding Affinity. The characteristic fluorescence change which accompanies MB binding can be used to estimate binding affinity (LePecq & Paoletti, 1967). Figure 5 shows the titration of free MB with nucleosomes or with linear

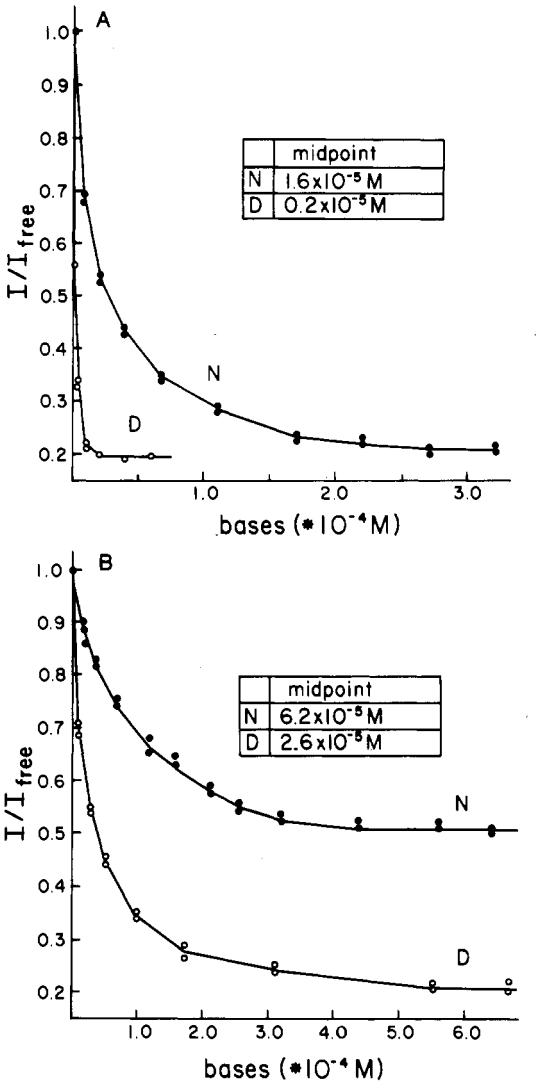

FIGURE 5: MB binding affinity as monitored by fluorescence. A dilute solution of MB (1.1×10^{-6} M) has been titrated with a concentrated solution of nucleosomes or linear 146 bp DNA in the same buffer. MB fluorescence is measured at each added substrate concentration and then normalized to its value for the free dye. The midpoint concentration specified as an insert to the plots corresponds to the substrate concentration in base equivalents required to induced half the maximal change of dye fluorescence. These midpoints are presented as a model-free measure of the binding process. (A) Titration in the presence of 10 mM Tris-HCl, pH 7.2, 4 °C: (top curve) nucleosome titration; (bottom curve) titration with linear, 146 bp DNA. (B) Titration in the presence of 10 mM Tris-HCl, pH 7.2, plus 300 μM $CaCl_2$, 4 °C: (top curve) nucleosome titration; (bottom curve) titration with linear 146 bp DNA. Note the similarity between nucleosome and DNA curves in the presence of 300 μM Ca^{2+}, which indicates that as monitored by its characteristic fluorescence change, MB binds to nucleosomes and to linear DNA with similar affinity in the presence of 300 μM Ca^{2+}.

146 bp DNA, as monitored by the fluorescence change which accompanies binding. As seen in Figure 5A, in the absence of added Ca^{2+}, MB binds to linear DNA with higher affinity than to nucleosomes. From a Scatchard analysis of these data (not shown), we calculate that the apparent affinity of MB for linear DNA is approximately 15 times that of nucleosomes in the absence of Ca^{2+} (the ratio of y-axis intercepts of the Scatchard plots is equal to 15).

On the other hand, in the presence of 300 μM free Ca^{2+} (Figure 5B), linear DNA and nucleosomes bind MB with similar apparent affinity. If the midpoints of these titration data are compared (inserts of Figure 5A,B), it is apparent that Ca^{2+} weakens the binding of MB to linear DNA but has a

Table I: Triplet Lifetime Decay[a]

sample	[Ca^{2+}] (μM)	fast component			slow component		
		A	k_q	α	A	k_q	α
MB	0	1	3×10^9	1			
MB/146	0				1	1.6×10^8	0.05
MB/146	600	0.38	6×10^8	0.2	0.67	1.5×10^8	0.05
MB/poly(dA)·poly(dT)	0				1	2.8×10^8	0.10
MB/poly(dG)·poly(dC)	0				1	6.4×10^7	0.02
MB/nucleosome	0	0.39	9.5×10^8	0.31	0.6	1.6×10^8	0.05
	100	0.58	1.2×10^9	0.40	0.46	1.6×10^8	0.05
	300	0.79	1.3×10^9	0.43	0.31	1.5×10^8	0.046
	450	0.82	1.3×10^9	0.43	0.25	1.4×10^8	0.05

[a] All measurements were performed at 4 °C at atmospheric pressure. Bimolecular rate constants (k_q) are standardized to 20 °C by using methods described elsewhere (Berkoff et al., 1986). A refers to the amplitude calculated from a fit of the data measured in 1.6 mM dissolved oxygen. Fits which lacked a significant second component lack an entry. Data for polynucleotide helices are from Berkoff et al. (1986). k_q is the measured bimolecular O_2 quench rate constant, calculated by measuring lifetimes at 1.6 mm O_2 and in argon-saturated solutions [see Berkoff et al. (1986) for details]. As described in the text, α is an accessibility parameter equal to the measured quench rate constant divided by that for free MB. In all instances, measurements have been made at a DNA or nucleosome substrate concentrations sufficient to bind MB to completion. For nucleosomes, the dye to particle ratio was 1.2. For DNA complexes, the dye to base pair ratio was 0.01. See the legend to Figure 6 for details.

smaller effect on overall binding affinity to nucleosomes.

Two important conclusions can be drawn from these data. First, in the presence of saturating Ca^{2+}, MB binding to nucleosomes is complete at all substrate concentrations above 5×10^{-4} M (bases). Since probe-dependent measurements described in this work have been made at substrate concentrations higher than 10^{-3} M, it is certain that unbound dye does not contribute to those data.

Second, since Ca^{2+} and MB are both cations, the trivial effect of binding Ca^{2+} is to weaken MB binding. Competition of that kind occurs when MB is bound to linear DNA but not when bound to nucleosomes. Failure to see a significant affinity decrease in nucleosomes is indirect evidence that Ca^{2+} alters MB binding by a process that cannot be understood in terms of ion competition alone.

Oxygen Quenching of the MB Triplet State. Solute quenching of dye probe excited states has been used extensively to monitor the accessibility of chromophores in macromolecules (Lakowcz & Weber, 1973). Recently, we have shown that oxygen quenching of the MB triplet state can be used in that way to provide a measure of the protection afforded by intercalation into a helix (Berkoff et al., 1986). The advantage of the method, relative to fluorescence quenching, is that oxygen (or another appropriate solute) can be used as a triplet quencher at a low concentration.

In Figure 6, we display curves which monitor the decay of the MB triplet state at 1.6 mM O_2. In the absence of added Ca^{2+} (Figure 6A, top curve), decay of the MB–nucleosome complex is multiphasic and can be characterized adequately as a sum of two similar exponential components (Table I). As we have discussed elsewhere, modest binding site heterogeneity of this kind is likely to result from base sequence dependent variation of intercalated MB complexes (Berkoff et al., 1986).

When MB–nucleosome complexes are titrated with Ca^{2+} (Figure 6A, lower curves), a significant fast decay component becomes evident, under conditions where 146 bp complexes show little effect (Figure 6B). The Ca^{2+} concentration dependence of the effect is as predicted from the Ca^{2+} binding data, reaching an end point at a concentration near 450 μM added Ca^{2+}. At that end point, the data are fit adequately as a sum of two very different exponential components (Figure 6A, curves through the data) with a ratio of fast to slow decay amplitudes equal to 3.3. Such a multiphasic decay process requires that there are at least two classes of MB bound to the nucleosome.

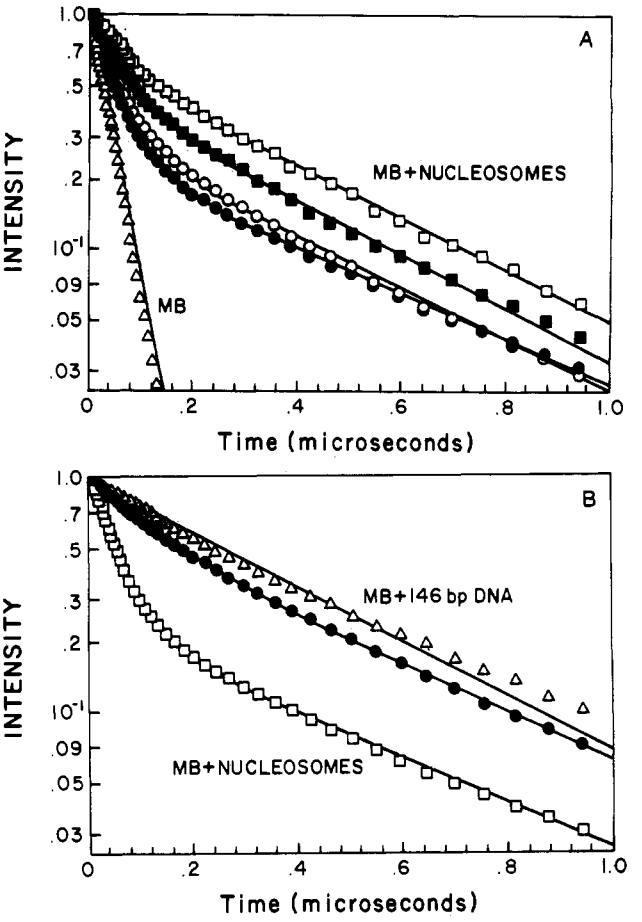

FIGURE 6: Lifetime measurements of the MB triplet state. Triplet state lifetime measurements have been performed as described under Materials and Methods. DNA or nucleosome complexes were prepared at 1.3×10^{-3} M (in bases) at a ratio of 1.2 dye per particle. Measurements were made at 4 °C in 10 mM Tris-HCl at equilibrium with atmospheric O_2. $CaCl_2$ was added as a concentrated stock solution. (A) Effect of Ca^{2+} on MB–nucleosome complexes: (△) free MB in Tris buffer; (□) MB–nucleosomes, 0 μM Ca^{2+}; (■) MB–nucleosomes at 100 μM Ca^{2+}; (○) MB–nucleosomes at 450 μM Ca^{2+}; (●) MB–nucleosomes at 800 μM Ca^{2+}. Solid lines through the nucleosome data refer to a two-exponential fit to the data (see Table I for those numerical fits). (B) Effect of Ca^{2+} on MB–146 bp DNA: (△) MB–DNA complexes, no added Ca^{2+} (the solid line corresponds to a single exponential fit to the data); (●) MB–DNA, 600 μM added Ca^{2+} (the solid line corresponds to a two-exponential fit to the data); (□) MB–nucleosome at 450 μM added Ca^{2+}.

We have measured O_2 quenching of the MB complex as a function of added Ca^{2+} concentration, using methods which

we describe elsewhere (Berkoff et al., 1986). Those data are cataloged in Table I. Three features of the quenching data should be emphasized.

First, the slower decay process which is detected in nucleosomes in the presence of Ca^{2+} (Figure 6A) is characterized by a quenching rate constant which is identical with the principal decay component of linear DNA. Second, the faster decay component which dominates decay in MB–nucleosome complexes in the presence of Ca^{2+} is quenched at a rate which is approximately twice that of the fastest 146 bp DNA component. Third, although adding Ca^{2+} to saturation increases the fraction of MB molecules bound to sites with a short lifetime, the quenching rate at those sites is not dependent upon Ca^{2+} ion concentration.

Together, those lifetime and quenching data suggest that in the Ca^{2+}-saturated nucleosome, bound MB molecules are partitioned into two principal kinetic classes: sites f, amounting to 76% of the bound probe with a characteristic O_2 quenching rate constant equal to 1.3×10^9 M^{-1} s^{-1} (Table I), and sites S, amounting to 23% of the probe, with a quenching rate constant equal to 0.15×10^9 M^{-1} s^{-1} (Table I). Sites S are very similar to MB binding sites on linear DNA, or MB sites in the Ca^{2+}-free nucleosome, but sites f are quite different.

Since O_2 quenching of the triplet state requires collisional contact with a dye probe (Berkoff et al., 1986), quenching rates can be used to calculate the fraction of dye surface area accessible to O_2 collision, i.e.

$$k_q/k_D = \alpha \qquad (2)$$

where k_D is the measured diffusion-limited quench rate constant for the free dye and k_q is the rate constant measured in a bound complex. The parameter α is useful in that it is a measure of the protection afforded by secondary structure at a binding site, yet is independent of any particular structure model. Oxygen quenching data have been cataloged in that way for nucleosome and 146 bp DNA complexes (Table I).

In the context of a model, α can be used to infer general features of binding site structure. Previously, we discussed one simple approximation in which an intercalated dye is modeled as occupying a wedge-shaped binding site opened to a full angle θ, i.e., for bases stacked parallel upon an intercalator such as MB, θ approaches zero (Berkoff et al., 1986). In such a model, we have proposed that O_2 can diffuse into contact with MB only if the intercalation site is opened. In that model, accessibility parameters and binding site geometry are simply related:

$$\alpha = \langle\theta^2\rangle^{1/2}/\pi \qquad (3)$$

where $\langle\theta^2\rangle^{1/2}$ is the root mean square angle which defines the shape of the (wedged) MB binding site (Berkoff et al., 1986).

When eq 3 is applied to quenching data for MB–146 bp DNA complexes, we calculate an average opening angle θ of 9° (Table I), which is within the range of values measured for synthetic DNA helices (Berkoff et al., 1986) and is as predicted from a consideration of spontaneous bending motions of a helix (Barkley & Zimm, 1979).

In Ca^{2+}-saturated nucleosome complexes, the slow component of MB decay (site S) is characterized by that same calculated angle (Table I). However, the more rapidly decaying class of bound MB is calculated to be within a site (site f) which is opened to 88°. Such a calculated angle is model dependent. However, the calculation may be meaningful in light of anisotropy decay data presented below.

Triplet Anisotropy Decay Measurements. Previously, we have shown that molecular motions experienced by intercalated MB are a useful measure of DNA flexibility in nucleosomes

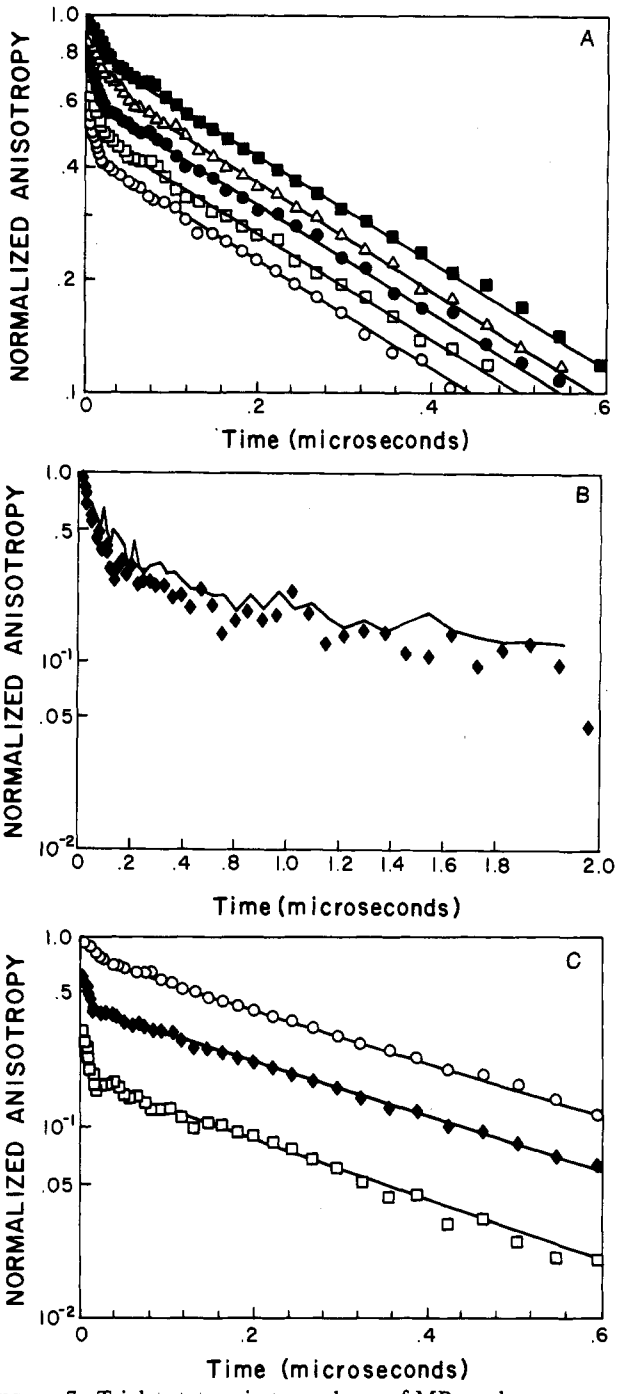

FIGURE 7: Triplet state anisotropy decay of MB–nucleosome complexes. Samples were prepared as in Figure 6. Measurements were made in argon-saturated solution at 4 °C. In each instance, decay data have been divided by 0.25 which is the intrinsic value of MB anisotropy measured in viscous media (see Materials and Methods for a discussion). (A) Triplet anisotropy decay of MB–nucleosome complexes: (■) 0 μM added Ca^{2+}; (△) 200 μM Ca^{2+}; (●) 400 μM added Ca^{2+}; (□) 600 μM added Ca^{2+}; (○) 800 μM added Ca^{2+}. (B) Triplet anisotropy decay of MB–146 bp DNA complexes: (solid line) no added Ca^{2+}; (♦) 800 μM added Ca^{2+}. (C) Calculated anisotropy decay data for MB bound to mobile, O_2-sensitive sites in the nucleosome. Data were generated by using eq 6, as described in the text. (○) Raw data for MB–nucleosomes at 0 μM Ca^{2+}; (♦) raw data for MB–nucleosomes at 800 μM Ca^{2+}; (□) corrected difference data. Solid lines are two-exponential fits to the data (see Table II for numerical fits).

(Wang et al., 1982). We also showed that the anisotropy decay method provides a sensitive measure of rotational tumbling of the nucleosome, from which nucleosome dimensions can be calculated accurately (Wang et al., 1982). The goal

Table II: Anisotropy Decay of Nucleosome Complexes[a]

sample	[Ca^{2+}] (μM)	A_f	γ_f (ns)	A_s	γ_s (ns)
MB/nucleosome	0	0.21	17	0.81	310
	200	0.24	16	0.70	304
	400	0.35	8	0.61	306
	600	0.43	8	0.51	312
	800	0.38	7	0.42	306
corrected MB/nucleosome	800	0.31	6	0.18	280

[a] MB/nucleosome complexes were measured under conditions described in the legend to Figure 7. Measured data have been normalized by dividing by 0.25. Decay curves were fit as a sum of two exponentials (see text). A and γ refer to the amplitude and time constant for each of the two decay components. Corrected MB/nucleosome refers to a two-exponential fit to the *calculated* anisotropy curve for the Ca^{2+}-dependent binding site (see text).

of experiments presented here is to determine how Ca^{2+} binding affects the dimensions of the nucleosome and to determine if DNA flexibility is altered by Ca^{2+} binding.

In Figure 7A, we display anisotropy decay curves of nucleosomes labeled with 1.2 MB molecules per particle. As we have determined previously for nucleosomes, the data are characterized by two components: a fast decay process which corresponds to local torsional motions of the DNA helix and a slower process which monitors overall tumbling of the nucleosome (Wang et al., 1982).

Ca^{2+} binding has a major effect upon the anisotropy decay of MB-tagged nucleosomes (Figure 7A, lower curves). Several features of qualitative importance should be noted from these data and from a two-exponential fit to the curves (Table II): (a) Ca^{2+} binding induces an increase in the rate and amplitude of the fast component of anisotropy decay. (b) The rate of anisotropy decay at long times is not affected by added Ca^{2+}. That slower decay process is a direct measurement of the overall tumbling of the particle (the rate varies as the diameter cubed). Therefore, without reference to any particular model, such Ca^{2+} independence suggests that the *overall dimensions of the nucleosome are not changed as a result of Ca^{2+} binding* and that Ca^{2+} binding in this concentration range does not give rise to nucleosome aggregation. Identical results were obtained when Tb^{3+} was substituted for Ca^{2+} (not shown). (c) The Ca^{2+} concentration dependence of the anisotropy data is qualitatively similar to that monitored by CD and by dye or ion probe fluorescence, i.e., as seen in Figure 7A, and as determined by other anisotropy experiments (not shown), the nucleosome transition monitored by MB is complete by 800 μM total Ca^{2+}, corresponding to a bound ion density and free Ca^{2+} concentration of 0.15 and 600 μM, respectively. (d) Bound Ca^{2+} ion has no effect on the anisotropy of linear DNA, over a 3-decade time range (Figure 7B). Independent of any particular kinetic model, those data suggest that Ca^{2+} binding to linear DNA does not alter helix flexibility or helix dimensions.

Since the faster decay process evident in the nucleosome data is due to motion of the dye probe, independent of overall nucleosome tumbling, the increase in the rate and amplitude of the fast component which results from Ca^{2+} binding suggests either that DNA in the particle has become very flexible or else that the bound dye probe is no longer held firmly at its binding site.

We favor the second explanation for two reasons. First, at the end point of the Ca^{2+}-induced transition (Table II), the time constant for the fast decay process has decreased to a value less than or equal to 7 ns (the resolution of our device). We find that no available theory for DNA flexibility can fit the amplitude or time scale of that decay process adequately. Second, as described previously, we have determined that in the presence of saturating Ca^{2+}, MB appears to partition into a second class of site with enhanced accessibility to O_2, as if it were positioned inside an open DNA binding site. In such a site, MB might experience large and fast librational motions.

In order to quantify anisotropy decay data in the context of these ideas, we have formulated a simple dynamic model which allows for two classes of MB binding site in the nucleosome: (1) site f, which is open (as deduced from O_2 quenching data), allowing for MB to wobble at its binding site over an angle θ; (2) site S, where MB is sandwiched firmly in the helix (as deduced from quenching data), experiencing only the relatively small torsional and bending motions predicted from the flexibility of a linear helix element.

For the purpose of calculation, let A_s and N_s refer to the absorbance and relative abundance of MB at rigid binding sites, and let A_f and N_f refer to the corresponding quantities for the mobile class of site. As suggested by the O_2 quenching data, we propose that MB is bound only to rigid sites in the absence of Ca^{2+} but in the presence of bound Ca^{2+} begins to partition between rigid and (newly created) mobile binding sites.

In order to proceed here, we have to make two simplifying assumptions. The first assumption we will make is that the absorption spectrum of the two species is the same. It is obvious from Figure 3 that this assumption is *not* correct, yet since the errors introduced by this simplification are on the order of 10% in amplitude, they are not enough to justify making further assumptions concerning the spectra of the two species. The second assumption we make is that the initial anisotropy of the two species is the same.

As Kinosoto and colleagues have discussed (Kawato & Kinosoto, 1981), the initial anisotropy is a function of the relative absorbance and the relative polarization of overlapping absorbance transitions. Therefore, our second assumption is equivalent to our first, with the added stipulation that a change of MB binding site structure does not alter the direction of transition dipole moments within the dye heterocycle.

In the context of those two simplifications, and in light of the two-site model which we have proposed, the calcium-induced changes in MB anisotropy decay curves must result from a redistribution of the dye between the two classes of nucleosome binding site.

For either of the two classes of bound MB which we have proposed, let $\Delta A = A_{\parallel} - A_{\perp}$ be the time-dependent linear dichroism contributed by each site in our measurements, and let $A = A_{\parallel} + 2A_{\perp}$ be the time-independent absorbance contribution from each site. In the context of the model, at any bound Ca^{2+} density, we can express the total measured anisotropy, $r(t)$, as a sum of those two terms:

$$r(t) = \frac{\Delta A_s + \Delta A_f}{A_f + A_s} \tag{4}$$

At this point, we take advantage of the two simplifications made earlier, i.e., that when bound to either site S or site f, MB has approximately the same absorbance and the same initial anisotropy. In light of those simplifications, it is easy to isolate the contribution of (mobile) Ca^{2+}-induced binding sites from the data:

$$r(t) = \frac{r_f(t)}{1 + F} + \frac{r_s(t)}{1 + 1/F} \tag{5}$$

where $F = N_s/N_f$, $r_f = \Delta A_f/A_f$, and $r_s = \Delta A_s/A_s$. Here $r_f(t)$ and $r_s(t)$ refer to the contribution of mobile and rigid sites to the total anisotropy signal. We have proposed that in the absence of Ca^{2+}, MB is bound exclusively to the rigid class of site. Therefore, when rearranged, eq 5 provides a simple

relation between the anisotropy in the presence of Ca^{2+} [$r(t)$] and the contribution of mobile sites to the data [$r_f(t)$], i.e.

$$r_f(t) = \left[r(t) - \frac{r_s^0(t)}{1 + 1/F} \right](1 + F) \quad (6)$$

Here, we define $r_s^0(t)$ to be the measured anisotropy in the absence of Ca^{2+}; i.e., the total signal in the absence of calcium is defined as resulting from MB binding to rigid sites.

In Figure 7C, we display such a calculation of $r_f(t)$, derived by subtracting anisotropy decay data at the two extremes of the Ca^{2+}-induced transition, i.e., r_s^0 at 0 μM and $r(t)$ at 800 μM Ca^{2+}. In this calculation, we have fixed the relative abundance (F) of MB binding sites to be 3.3, as specified by the relative abundance of open and protected sites in O_2 quenching measurements. A two-exponential fit of that calculated decay curve is presented graphically in Figure 7C and numerically in Table II. In the context of the calculation as we have performed it, the fast component of such a two-exponential fit to the corrected data specifies the amplitude and time constant for dye probe motion at the (mobile) Ca^{2+}-induced MB binding site. The slow component should correspond to overall tumbling of the nucleosome, as monitored at that MB site. Overall tumbling is a property of all sites of the nucleosome and therefore should not be changed by calculation of the kind we have made in Figure 7C. That invariance is borne out by the data.

The mathematical model we have employed to evaluate anisotropy decay at mobile Ca^{2+}-induced sites is described by Kinosita (Kawato & Kinosita, 1981). This model describes wobbling of the dye probe as diffusional motion over a cone-shaped space, opened to a full angle of 2θ:

$$r_\infty/r_0 = [0.5(\cos\theta)(1 + \cos\theta)]^2 \quad (7)$$

In the context of that expression, r_∞ is equal to the amplitude contribution of overall tumbling to the corrected data when extrapolated to zero time, while r_0 is the measured value of the data at $t = 0$. The ratio r_∞/r_0 calculated from the corrected data is 0.18 (Table II), from which we calculate an angle 2θ equal to 100°.

The Kinosita expression constitutes a broad approximation to real dynamics; however, no alternative formalism is available at this time. Nevertheless, amplitudes calculated in the context of such a model serve to rough out an approximate scale to the motions which are being monitored. Rather than focus on that modeling limitation, it is more important to recognize that the Kinosita model accounts for the motion of only one transition dipole, while the MB signal which we monitor almost certainly arises from the superposition of signals from two perpendicular transition moments.

If, as suggested from O_2 quenching measurements, MB is free to wobble within a wedge-shaped binding site, a dipole directed parallel to the wedge could remain motionless, even if a perpendicular moment were fluctuating over the entire wedge angle. Again, for expediency and in the absence of a more detailed theory for anisotropic motion, we will ignore these complications and assume simple conelike diffusion.

In spite of the simplification we have employed, the similarity between that (motional) estimate of binding site geometry (100°) and the estimate derived from oxygen quenching (88°) is interesting and will be discussed below.

Discussion

Work presented here suggests that when bound to a nucleosome core particle, Ca^{2+} can induce a change in the physical properties of the folded DNA helix. The data we have presented are not sufficient to establish the molecular details of the transition we have monitored in an unambiguous way. However, the data do place major limitations upon the range of consistent explanations. Below, we note those constraints:

(1) DNA is wrapped as a superhelix on the outside of a nucleosome, forming its outer dimension (Richmond et al., 1984). Since Ca^{2+} binding does not alter those dimensions (Figure 7A), the pitch associated with superhelical folding cannot change appreciably as a result of Ca^{2+} binding to the nucleosome. Moreover, the ion independence of the slow anisotropy decay component (Figure 7A) rigorously confirms that Ca^{2+} binding does not induce aggregation of nucleosomes in the concentration range we have studied.

(2) Ca^{2+} binding to the nucleosome, as measured thermodynamically (Figure 1A), and Tb^{3+} binding, as measured spectroscopically (Figure 1B), appear to be biphasic, displaying one class of binding site at a density lower than 15 or 20 per nucleosome and a second class in the range from 20 to 40 per particle. On the basis of the high efficiency of DNA to Tb^{3+} energy transfer (Figure 1B), it is very likely that the first high-affinity Tb^{3+} binding site is on the DNA helix. By inference, we conclude that the equivalent Ca^{2+} binding site is also on DNA.

(3) DNA structure change can be detected in the nucleosome by CD spectroscopy (Figure 2). The dose dependence of these changes is as expected from binding equilibria, resulting in a 50% decrease in ellipticity at 280 nm. The measured change suggests that when integrated over the whole particle, Ca^{2+} binding results in a change of base stacking interactions in the helix.

(4) Intercalating dye probe molecules continue to bind tightly to the Ca^{2+}-saturated nucleosome. Although the ion-induced transition is accompanied by a change of MB absorbance (Figure 3) and fluorescence (Figure 4), the fluorescence and absorbance of the bound dye are qualitatively similar to those of its intercalated complex with linear DNA. On the basis of such spectral similarity, and the observation that the dye binds tightly to the nucleosome in the presence of Ca^{2+} (Figure 5), we conclude that the nucleosome retains many sites for dye probe intercalation when in the ion-saturated state. Such an outcome excludes the possibility that the dye probes are binding to one or two rare sites (such as the ends of a helix) since such few hypothetical sites would have to possess an unreasonably high binding affinity.

(5) Anisotropy decay and O_2 quenching measurements suggest that there are two distinct classes of bound MB in the ion-saturated nucleosome: one which is very similar to ordinary intercalation and another which experiences large-scale librational motion at its binding site (Figure 7) and, as a result, is accessible to oxygen quenching (Figure 6).

(6) None of the Ca^{2+}-induced changes we have monitored can be detected on linear DNA fragments or on nucleosomes in the presence of excess Na^+. Preliminary work (Figure 4) suggests that divalent metals such as Mg^{2+} can produce similar effects. We have also tested two multiply charged oligopeptides, Lys_2 and Lys_4, and find that they have no effect on nucleosome structure, as monitored by CD or MB fluorescence (not shown). However, in preliminary experiments, the organometallic complex $[Co(NH_3)_6]^{3+}$ appears to be as effective as Tb^{3+} (not shown).

Consequently, we believe that the phenomenon we have monitored is not specific to Ca^{2+} but is a more general property of multivalent ion binding to nucleosomes.

Working Hypothesis To Correlate Ca^{2+} Binding Data. When an elastic body is subjected to bending stress, the strain (physical deformation) which results can be biphasic: at low

stress, elastic rods tend to bend in a smooth continuous fashion; at high stress, rods tend to kink (bend discontinuously) or else engage in irreversible changes such as fracture or plastic deformation (Eisenstadt, 1971). The critical stress at which the bending mechanism changes is different for different materials. However, for stiff elastic rods, the onset of such a change may be expected when the radius of bending curvature is reduced to a value near the rod diameter, d.

For a nucleosome, r/d is equal to 1.7 (using r = 43 Å and d = 25 Å); therefore, the general properties of elastic materials would predict that a DNA helix may be stressed enough to equilibrate between different bent structures.

On the basis of that general observation, we propose the following working hypothesis to interpret the data we have presented. We suggest that in the absence of multivalent ions such as Ca^{2+}, DNA in the nucleosome is bent smoothly so that the angular deformation and local nucleotide structure change attendant to folding is dissipated continuously over the helix. On the basis of energy considerations, Levitt has concluded the DNA can be folded in that way with only a modest local change of nucleotide geometry (Levitt, 1978). Consequently, base stacking interactions and the capacity of such a smoothly folded helix to bind ligands may be very similar to that measured for a linear DNA helix under the same conditions.

Next, we propose that as a result of Ca^{2+} binding (and perhaps the binding of other multivalent ions) DNA in the nucleosome undergoes a transition from a smoothly folded to a kinked helix geometry. In the context of a theory for elastic rods, the effect of binding Ca^{2+} can be viewed as shifting the critical stress required to induce a smooth to discontinuous folding transition in a DNA helix.

In terms of a chemical equilibrium, the effect of binding Ca^{2+} can be viewed as arising because Ca^{2+} binds specifically to one or more features peculiar to the kinked helix geometry. As a result of that local binding event, Ca^{2+} may either induce the formation of a kinked geometry or else trap such sites after they have formed (an allosteric explanation similar to that used to describe O_2 binding to hemoglobin).

Several models for a DNA kink have appeared in the literature (Crick & Klug, 1975; Sobell et al., 1977; Zhurkin et al., 1979). Among those models, we have concluded that the kinked helix structure proposed by Crick and Klug provides the closest correspondence between our data and such a working hypothesis (Crick & Klug, 1975). In their structure model, DNA is bent approximately 90°, due to rotation about two $C_{4'}$–$C_{5'}$ bonds at the kink site. As a result, the major helix groove opens to produce a 90°, wedge-shaped site in the helix, and the minor groove is compressed. To wrap DNA in a nucleosome as a series of those kinks, Crick and Klug have pointed out that they must be positioned at 20-base intervals, separated by a 20-base-long stretch of linear DNA helix (Krick & Klug, 1975). They predict six such kinks per $1^3/_4$ superhelical turns of DNA in the particle.

We present a wire model of such a kink in Figure 8. In addition to the prominent, wedge-shaped discontinuity at the kink, it is interesting to note that as a result of the bend, phosphates at the edge of the (collapsed) minor groove are brought close together. Below, we interpret our experiments in the context of this model.

Ion Binding. The model is interesting in that, as a result of rotating $C_{4'}$–$C_{5'}$ bonds at a kink site, three or perhaps four phosphate residues at the rim of the minor groove are brought close together. The two phosphates which form the site of closest contact are marked by spheres. It is expected that closely spaced phosphate oxygens of that kind might bind tightly to a multivalent ion. As many as 2 Ca^{2+} or Tb^{3+} could bind to a cluster of 4 phosphates, which would amount to 12 tightly bound ions per particle (0.04 per base) if such kinks are separated by 20-base intervals. As noted in Figure 1, we have identified a class of high-affinity Ca^{2+} binding sites at densities below 0.05 per base. We suggest that binding of that kind occurs at the phosphate cluster. The excess free energy of binding to such a cluster, compared to isolated phosphates in a linear helix, may be why an ion must be multivalent in order to drive the smooth to kinked helix equilibrium.

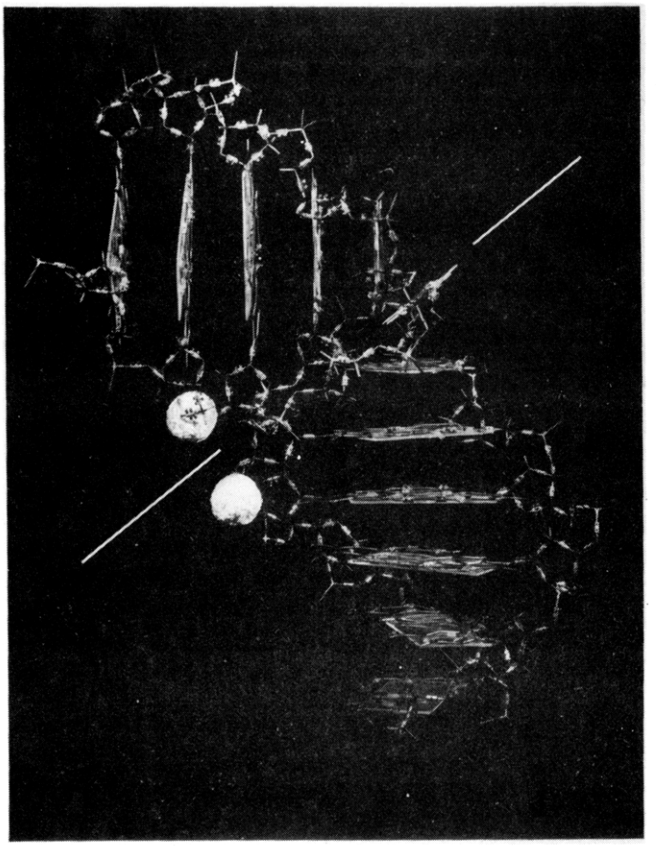

FIGURE 8: Model for ion-induced kinks in a nucleosome. Crick and Klug have shown that by rotating the $C_{4'}$–$C_{5'}$ bonds at a base pair, a 90° bend will be introduced into an otherwise undistorted DNA duplex (Crick & Klug, 1975). We have built such a structure at the center of a 10 base pair long B DNA duplex. Several important features of this structure are displayed in Figure 8. As Crick and Klug discuss, the major groove of the helix opens and the rim of the minor groove collapses upon itself as a result of those two bond rotations. It is important to emphasize that a kinked structure of this kind creates *two* new structure features on DNA: unstacked bases at the kink and a collapsed minor helix groove. Phosphates at the rim of the collapsed minor groove come within 2 Å of each other (the two closest phosphates are marked by spheres in Figure 8). We have proposed that multivalent ions may bind to this second class of feature by chelating that cluster of phosphate oxygens. Such a structure possesses a pseudodiad axis which we have marked by a line (the kink is viewed from the side, parallel to the diad axis in this projection). Phosphates in the minor groove are symmetrically disposed relative to that diad. Therefore, if a multivalent ion were bound to clustered phosphates at the kink, it would be positioned equidistant from two segments of helix (segments 3 bases to either side of the kink itself). A second site created by a kink transition is at the bend. Two base pairs to either side of the kink separate and local base pair diads become perpendicular. That deformation produces a wedge-shaped site within the helix stack, which we have proposed to be a site where an intercalator binds to this structure. In Figure 8, we have positioned methylene blue at this site, with its long axis parallel to the long axis of the two base pairs which flank the kink. In the figure, we have oriented the dye plane so that its short axis is coincident with the diad axis of the kink. However, as described in the text, our data suggest that the short dye axis wobbles at this binding site over the entire 90° angular range to which it has access.

In an alternative model, Sobell and colleagues have described how DNA can kink in a more modest fashion (a 45° rather than a 90° bend, which opens toward the minor groove, thereby compressing the major helix groove at the kink site). Upon inspection of that model (Sobell et al., 1976), we have noticed that because the major groove is wide and because the binding deformation is smaller, phosphates which rim the major groove are not compressed together upon forming a Sobell-type kink. For that reason, it is difficult to propose a mechanism for coupling multivalent ion binding to the formation of kinks or bends of that kind which compress the (wide) major helix groove.

Terbium Energy Transfer. As noted in Figure 8, there are two DNA base pairs equidistant from the phosphate cluster in a kink. In the model, each of those two base pairs resides within a helix region which is similar to unstressed B DNA. The optical properties of those bases should be very similar to those of bases in a linear helix. In that instance, the characteristic distance for half-maximal energy transfer to Tb^{3+} should be comparable to that for Tb^{3+} bound to linear DNA. With that simplification, Tb^{3+} fluorescence at a kink binding site can be related to fluorescence measured when bound to linear DNA, by simply adding up the number of base to Tb^{3+} interactions.

As indicated by the model in Figure 8, the base to Tb^{3+} separation at a phosphate cluster in a kink is indistinguishable from the base to Tb^{3+} separation in linear DNA. Therefore, Tb^{3+} fluorescence in the cluster should be twice that of linear DNA, independent of the detailed mechanism of base to Tb^{3+} energy transfer. The measured value (Figure 1B) is 2.5. Considering the simplifications we have employed, we believe that the correspondence with the model is very good.

CD. First-order CD theory predicts that base unstacking, as at a kink, should reduce DNA ellipticity at 280 nm (Bush, 1974). Therefore, the Ca^{2+}-dependent ellipticity decrease which we detect (Figure 2) is consistent with the kinked helix model. However, we believe a more detailed application of CD theory may be inappropriate.

MB Hypochromism. We propose that MB binds directly to kink sites which form in the nucleosome. As displayed in Figure 8, when bound in that fashion, the long axis of the dye remains parallel and in close proximity to the base planes which form the kink. On the other hand, the short dye axis (which projects outward from the wedge-shaped site) cannot remain in contact with both base neighbors. In the Ca^{2+}-saturated nucleosome, absorbance measurements indicate that the one dye transition moment experiences strong stacking but the other is nearly unstacked compared to a linear MB–DNA complex (Figure 3). The model we have proposed explains those hypochromism data quite adequately if, as is likely, the 620-nm MB absorbance transition is directed along the short dye axis.

O_2 Quenching and Anisotropy Decay Measurements. The simple geometric models which we have used to interpret O_2 quenching and anisotropy decay data predict that, as a result of Ca^{2+} binding to nucleosomes, approximately 77% of bound MB molecules become associated with a site which is opened and may be modeled as a wedge or cone with an opening angle near 90°. As seen in Figure 8, the kink structure which we have proposed does form a wedge-shaped site with an opening angle equal to 90°. The more modest kink structure proposed by Sobell et al. also predicts that kink sites will be wedge shaped, but opened to a smaller angle (45°). Independent of any particular kinetic model, we feel that the O_2 quenching and anisotropy decay measurements we have made on nucleosomes are not consistent with an intercalator binding site which is as constrained as predicted by the Sobell model. Therefore, we consider the quenching and anisotropy decay data to be good evidence in favor of MB binding to ion-induced kinks of the kind described by Crick and Klug.

Clearly, additional work is required to test and modify the model we have described. However, several independent lines of evidence suggest that general features of such a model may have validity:

(a) High-resolution nuclease mapping experiments with DNase II, as described by Lutter (Lutter, 1981) and Sollner-Webb (Sollner-Webb et al., 1978), suggest that the distribution of nuclease cutting sites in the nucleosome changes significantly in the presence of 5 mM $MgCl_2$, compared to Mg^{2+}-free solutions. Preliminary work in our laboratory (not shown) shows that the nucleosome has undergone the ion-induced structure change in those Mg^{2+}-containing reaction solutions. Therefore, we suggest that the cutting rate change which is detected in those nuclease digestion experiments may reflect the DNA conformation change we have described.

(b) On the basis of substantial biophysical experimention—^{31}P NMR (Klevan et al., 1979), ^{1}H NMR (Feigon & Kearns, 1979), and anisotropy decay (Wang et al., 1982; Watanabe et al., 1983)—it has been concluded that the physical properties of DNA in the nucleosome are similar to those of linear DNA helices. Those studies were performed in the *absence* of added multivalent ions or else were performed at substrate and ion concentrations which were high enough that multivalent ion binding could not be studied, due to aggregation processes (Klevan et al., 1979). Consequently, we believe that those structure studies are consistent with the model we have proposed, because they confirm that in the absence of multivalent ions, DNA in the nucleosome appears to be folded as a uniform helix, free from discontinuities which could be detected by NMR or other methods.

(c) DNA in the available nucleosome crystal structure displays smoothly deformed and discontinuously deformed (kinked) helix regions within the same particle (Richmond et al., 1984). Although it is difficult to relate structure polymorphism in the solid state to a solution state equilibrium, we suggest that the mixed pattern of folding which is detected in the crystal provides evidence that the absolute energy of a discontinuously bent helix can be similar to that of smoothly bent DNA (i.e., they can coexist in the same crystal form).

However, as Richmond and colleagues have pointed out (Richmond et al., 1984), an analysis of their 7-Å nucleosome structure suggests that the discontinuities which they detect do not appear to be similar to any of the available models for a kink (including that described by Crick and Klug). That observation is the strongest piece of evidence against the model we have proposed. Therefore, in the absence of more detailed structure information, we conclude that either the kinked structure detected in crystals is different from that which occurs in the solution state or else the close correspondence between our data and the Crick/Klug model for a kink is fortuitous. Higher resolution biochemical and biophysical work, now in progress, should discriminate between those alternatives.

However, for now it is sufficient to emphasize the general implications of the model. Although we have focused upon the effects of Ca^{2+} binding, preliminary data (Figure 4 and elsewhere) suggest that Mg^{2+} and other multivalents are capable of inducing the structure transition we have detected in the micromolar to millimolar concentration range. It is well-known that divalent ion concentration is controlled in cells

(Mg^{2+} concentration is maintained at or near millimolar) which raises the interesting possibility that in the nucleus the structural equilibrium which we have detected may be positioned near its midpoint.

Near such a midpoint, binding of effector molecules, chemical modification of histone contacts with DNA, or site-dependent variation of the DNA sequence which is folded as a nucleosome could each have an effect on the smooth to kinked helix equilibrium. Therefore, on the basis of such equilibrium concepts, it is interesting to consider the possibility that due to time-dependent changes in effector or divalent ion concentration, the secondary structure of DNA in genes might change from a smooth to a kinked helix geometry.

Alternately, site-dependent variation in DNA sequence or histone composition suggests that DNA secondary structure within a genome might vary in a site-specific manner, if indeed there are DNA segments which vary in their ability to assume a kinked helix (as opposed to a smoothly bent) structure.

The functional importance of kinks in a nucleosome remains to be elucidated. Recently, however, in other contexts it has been suggested that bending of DNA helices may be intrinsic to the expression and replication of genes (Wu & Cruthers, 1984; Makherjee et al., 1985).

From an equilibrium point of view, it is obvious that if a kink must form at a protein binding site, a preexisting equilibrium between a smooth and kinked helix geometry could regulate the binding event allosterically (much as a preexisting conformation equilibrium in hemoglobin is thought to regulate binding of its ligands). It remains to be determined if allosteric equilibrium in the nucleosome (mediated by ion binding) can be manipulated during the course of gene regulation.

Registry No. Ca, 7440-70-2; methylene blue, 61-73-4.

References

Albert, A. (1966) *The Acridines*, Edward Arnold Publishers, Ltd., London.

Austin, R. H., & LeGrange, J. D. (1985) *Rev. Sci. Instrum. 56*, 630–631.

Barkley, M. D., & Zimm, B. H. (1979) *J. Chem. Phys. 79*, 2991–3007.

Berkoff, B., Hogan, M. E., LeGrange, J., & Austin, R. H. (1986) *Biopolymers 25*, 307–316.

Bush, C. A. (1974) in *Basic Principles in Nucleic Acid Chemistry* (Tso, P. O. P., Ed.) p 92, Academic Press, New York.

Clement, R. M., Sturm, J., & Daune, M. P. (1973) *Biopolymers 12*, 405–421.

Cowman, M. K., & Fasman, G. D. (1978) *Proc. Natl. Acad. Sci. U.S.A. 75*, 4759–4763.

Crick, F. H. C., & Klug, A. (1975) *Nature (London) 255*, 530–533.

Eisenstadt, M. M. (1971) *Introduction to the Mechanical Properties of Solids*, p 187, Macmillan, New York.

Feigon J., & Kearns, D. R (1979) *Nucleic Acids Res. 6*, 2327–2337.

Friedman, R. A., & Manning, G. S. (1984) *Biopolymers 23*, 2671–2714.

Geladē, El., & De Schryver, F. C. (1984) *J. Am. Chem. Soc. 106*, 5871–5875.

Horrocks, W. D., Rhee, M.-J., Snyder, A. P., & Sudnock, D. K. (1980) *J. Am. Chem. Soc. 102*, 3650–3652.

Kawato, S., & Kinosita, K. (1981) *Biophys. J. 36*, 277–296.

Kayne, M. S., & Cohn, M. (1974) *Biochemistry 13*, 4159–4165.

Kern, J., & Doerr, F. (1961) *Z. Naturforsch., A: Astrophys., Phys. Phys. Chem. 16A*, 363–366.

Klevan, L., Armitage, I. M., & Crothers, D. M. (1979) *Nucleic Acids Res. 6*, 1607–1616.

Kovacic, R. T., & Van Holde, K. E. (1977) *Biochemistry 16*, 1470–1498.

Lakowcz, J. R., & Weber, G. (1973) *Biochemistry 12*, 4161–4170.

Landau, L., & Lifshitz, E. M. (1958) *Statistical Physics*, Addison-Wesley, Reading, MA.

LePecq, J. B., & Paoletti, C. (1967) *J. Mol. Biol. 27*, 87–106.

Levitt, M. (1978) *Proc. Natl. Acad. Sci. U.S.A. 75*, 640–644.

Lutter, L. C. (1981) *Nucleic Acids Res. 9*, 4251–4265.

Martin, R. B. (1983) in *Metal ions in Biology* (Spiro, T. G., Ed.) Chapter 6, Wiley, New York.

McGhee, J. D., & Felsenfeld, G. (1980) *Annu. Rev. Biochem. 49*, 1115–1196.

Mukherijee, S., Patel, I., & Bastia, D. (1985) *Cell (Cambridge, Mass.) 43*, 189–197.

Platt, J. R. (1949) *J. Chem. Phys. 17*, 484–495.

Prendergast, F G., Lu, J., & Callahan, P. J. (1983) *J. Biol. Chem. 258*, 4075–4078.

Richmond, T. J., Finch, J. T., Rushton, B., Rhodes, D., & Klug, A. (1984) *Nature (London) 311*, 532–537.

Sobell, H. M., Tsai, C. C., Jain, S. C., & Gilbert, S. G. (1976) *Proc. Natl. Acad. Sci. U.S.A. 73*, 3068–3072.

Sollner-Webb, B., Melchior, W., & Felsenfeld, G. (1978) *Cell (Cambridge, Mass.) 14*, 611–627.

Southwell, R. V. (1936) *Theory of Elasticity*, Clarendon Press, Oxford, Great Britain.

Stryer, L., Thomas, D. D., & Meares, C. F. (1982) *Annu. Rev. Biophys. Bioeng. 11*, 203–222.

Topal, M. D., & Fresco, J. R. (1980) *Biochemistry 19*, 5531–5536.

Wang, N. C., Hogan, M. E., & Austin, R. H. (1982) *Proc. Natl. Acad. Sci. U.S.A. 79*, 5896–5900.

Watanabe, K., Iso, K., & Nakano, T. (1983) *Biochemistry 22*, 6018–6026.

Wittwer, A., & Zanker, V. (1959) *Z. Phys. Chem. (Leipzig) 22*, 417–439.

Wu, H. M., & Crothers, D. M. (1984) *Nature (London) 308*, 509–513.

Wu, H. M., Dattagupta, N., Hogan, M. E., & Crothers, D. M. (1980) *Biochemistry 19*, 626–634.

Zhurkin, V. B., Lysov, Y. P., & Ivanov, V. I. (1979) *Nucleic Acids Res. 7*, 1081–1096.